Available online at www.sciencedirect.com
SCIENCE DIRECT®
International Journal of Heat and Mass Transfer 48 (2005) 5338–5353
International Journal of HEAT and MASS TRANSFER
www.elsevier.com/locate/ijhmt

Modelling of multi-component gas flows in capillaries and porous solids

J.B. Young *, B. Todd

Hopkinson Laboratory, Cambridge University, Engineering Department, Trumpington Street, Cambridge CB2 1PZ, UK

Received 2 March 2005
Available online 6 October 2005

Abstract

The paper presents a derivation of the governing equations for multi-component convective-diffusive flow in capillaries and porous solids starting from a well-defined model and clear assumptions. The solution for the continuum regime is discussed in detail including a derivation of the diffusion slip boundary condition based on an improved momentum transfer theory. The Stefan–Maxwell species momentum equations are also re-examined and important distinctions made between the local and tube-averaged equations. An equation for the pressure gradient is derived and some examples of binary flows in capillaries are discussed. The theory for free-molecule flow is standard but the equations are recast into a form identical to the continuum equations which suggests an obvious method of interpolation for flow at arbitrary Knudsen number. There are no problems concerning viscous terms which have marred other derivations. The extension to flow in porous bodies is achieved by introducing a porosity–tortuosity factor but, unlike other treatments, this parameter is not absorbed into the gas diffusivities and flow permeability. It can then be eliminated from all but one of the equations and, with appropriate boundary conditions, the flux ratios can be obtained in terms of a mean pore radius only. The porosity–tortuosity parameter simply controls the absolute flux level and is best interpreted as a length scale-factor. The theory is applied with success to the prediction of some experimental data for helium–argon counter-diffusion and it is shown that, contrary to common belief, the mean pore radius is well-defined by flux ratio measurements if these are made with non-zero pressure differences.

1. Introduction

This paper deals with the theory of multi-component gas transport in capillaries and porous solids. The engineering importance of the subject is evident from the large number of papers published over the last half century, particularly in the field of catalysed reactive flows. A recent research area, of particular interest to the authors, is solid oxide fuel cell technology where diffusion of fuel gas components and reaction products through the electrodes and porous ceramic support structure can be a limiting factor in the electro-chemical operation of the devices [1].

The two main theories in practical use are the dusty gas model (DGM) and the mean pore transport model (MPTM). The DGM was introduced by Evans et al. [2,3] and these two papers provide an account of the theory which is clearer and more well-balanced than the later, more frequently-cited monograph by Mason and Malinauskas [4]. The MPTM is associated with the work

* Corresponding author. Tel.: +44 (0)1223 330263.
E-mail address: jby@eng.cam.ac.uk (J.B. Young).

0017-9310/$ - see front matter © 2005 Elsevier Ltd. All rights reserved.
doi:10.1016/j.ijheatmasstransfer.2005.07.034

Nomenclature

A	coefficient in pressure gradient equation
c	molar density
D_A	flow coefficient at arbitrary Kn
D_B	binary diffusion coefficient
D_K	Knudsen flow coefficient
f	diffuse reflection coefficient
G	mass flux (per unit cross-sectional area)
J	molar flux (per unit cross-sectional area)
K	permeability
Kn	Knudsen number
M	molar mass
p	pressure
R	tube or mean pore radius
R_g	molar gas constant
r	radial co-ordinate
T	temperature
u, v	velocities in the mass and molar systems
$\bar{w}$	mean molecular random speed
X	mole fraction
Y	mass fraction
y	distance from wall ($R - r$)
z	distance through porous slab
ε	porosity
λ	mean free path of a gas molecule
μ	dynamic viscosity
ρ	mass density
τ	tortuosity
ξ	streamwise co-ordinate

Subscripts

C	continuum flow $Kn \to 0$
K	free-molecule flow $Kn \to \infty$
conv	convective component
diff	diffusive component
m	mass- or molar-mean
r, s	gas species r, s
w	evaluated at the tube wall

of Rothwell [5], Schneider [6], Arnost and Schneider [7] and others. The two theories are based on completely different physical models but, remarkably, the resulting equations are almost the same. A comparison can be found in the monograph by Jackson [8] and a recent appraisal, highly critical of the formalism of the DGM, is given by Kerkhof [9]. In the same paper Kerkhof proposes a modified MPTM theory called the binary friction model (BFM) and in Kerkhof et al. [10] yet another version, the velocity profile model (VPM), is introduced.

Unfortunately, none of these authors have been able to resolve the problem of algebraic complexity which besets the subject and causes serious difficulties of understanding. Everyone, it seems, has his own set of working equations and it appears to be a characteristic of the subject that the physical bases and assumptions somehow get lost in the development, with the result that it is extremely difficult to make informed comparisons between the different formulations. The present paper is an attempt to improve the situation by establishing a baseline theory with a clear derivation. Interestingly, the resulting mathematical simplification provides new insight and a physical interpretation which is quite different from the traditional way of visualising diffusive flow in porous solids. The new theory is related to the MPTM and BFM but is referred to here as the cylindrical pore interpolation model (CPIM) to emphasise the differences. Introducing yet another acronym into an already well-endowed field is undeniably presumptuous but the subject is in need of clarification and it is hoped that the CPIM will help to fulfill this objective.

Most applications of diffusive flow in porous media involve chemical reactions but these are not considered and the flow is assumed to be non-reacting and isothermal. Surface diffusion along the walls of the pores is also neglected. These and other complexities can be added at a later stage but the emphasis here is on simplicity and physical understanding.

2. The competing theories

The DGM of Evans et al. [2,3] starts from the assumption that the flow of a gas mixture through a porous solid is similar to the flow through a random array of solid spheres. The kinetic theory of gases is then used to establish the governing equations, the spheres being treated as an extra species of high molecular mass and large size, held in place by external forces. There are problems both with the physical model and the mathematical development and some of these have recently been highlighted by the careful deconstruction work of Kerkhof [9]. The present authors agree with Kerkhof's analysis and have rejected the DGM as a suitable foundation on which to construct a viable theory.

In contrast, the MPTM, BFM and VPM are all based on much sounder physics. Each model differs in important details but the common starting points are the analytical solutions for continuum, slip and free-molecule flow in straight capillary tubes. Equations for flow at transitional Knudsen numbers are obtained by interpolation and the *porosity* and *tortuosity* of the medium

are represented by empirical factors, sometimes in a rather arbitrary way.

This general description serves equally well for the CPIM of the present paper. However, the CPIM is differentiated from its competitors by a rigorous treatment of continuum flow, a clearer interpolation procedure for transitional flow, and a compact form of the working equations which helps to clarify the rôles of the governing parameters. MPTM theory is not standardised and different forms appear in the literature. Sometimes this is because the model assumptions are genuinely different but often it is because of unclear physical foundations or errors of derivation stemming from imprecise flux definitions, mass-molar transformation errors, incorrect treatment of the *viscous-flow* term and so-on. The CPIM theory, it is hoped, is at least unambiguous in its derivation from clear basic assumptions.

3. Definitions of fluxes and velocities

At the outset, it is important to define the various fluxes and velocities consistently. Many authors omit this essential first step with the result that ambiguity creeps into their work. In this paper, the standard decomposition for convective-diffusive flows is used as described in Spalding [11] and many other textbooks.

Let ρ_s and c_s be the mass and molar densities of gas species-s and let Y_s and X_s be the mass and mole fractions. If ρ and c are the mass and molar densities of the gas mixture, then

$$\rho_s = Y_s\rho, \quad \sum \rho_s = \rho, \quad \sum Y_s = 1 \tag{1a}$$

$$c_s = X_s c, \quad \sum c_s = c, \quad \sum X_s = 1 \tag{1b}$$

where the summations with respect to s are over all N species present.

All flows are assumed to be in straight cylindrical pores (with distance ξ measured along the pore) so vector notation is not required. Let G_s and J_s be the total mass and molar fluxes of species-s in the ξ-direction (the term *flux* means flow per unit cross-sectional area). It should be noted that G_s and J_s vary with radius r and do *not* represent pore-averaged values. The total mass and molar fluxes, G and J, also vary with r and are given by

$$G = \sum G_s \tag{2a}$$

$$J = \sum J_s \tag{2b}$$

The G_s and J_s are now decomposed into convective and diffusive parts. The convective fluxes are *defined* by the relations $G_{\mathrm{conv},s} = Y_s G$ and $J_{\mathrm{conv},s} = X_s J$ and this definition ensures that the diffusive fluxes $G_{\mathrm{diff},s}$ and $J_{\mathrm{diff},s}$ always sum to zero. Thus:

$$G_s = Y_s G + G_{\mathrm{diff},s} \quad \left(\sum G_{\mathrm{diff},s} = 0\right) \tag{3a}$$

$$J_s = X_s J + J_{\mathrm{diff},s} \quad \left(\sum J_{\mathrm{diff},s} = 0\right) \tag{3b}$$

Correct conversion between mass and molar forms is very important. If M_s is the molar mass of species-s, then $G_s = M_s J_s$ but, in general, $G_{\mathrm{conv},s} \neq M_s J_{\mathrm{conv},s}$ and $G_{\mathrm{diff},s} \neq M_s J_{\mathrm{diff},s}$. Also, if $M = \sum M_s X_s$ is the mean molar mass of the mixture, then in general $G \neq MJ$.

Various velocities can be defined in relation to the fluxes. Thus, u_s and v_s (the total mass/molar velocity of species-s), $u_{\mathrm{diff},s}$ and $v_{\mathrm{diff},s}$ (the mass/molar diffusion velocity of species-s) and u_m and v_m (the mass/molar mean velocity) are *defined* by

$$G_s = \rho_s u_s \quad J_s = c_s v_s \tag{4a}$$

$$G_{\mathrm{diff},s} = \rho_s u_{\mathrm{diff},s} \quad J_{\mathrm{diff},s} = c_s v_{\mathrm{diff},s} \tag{4b}$$

$$G = \rho u_m \quad J = c v_m \tag{4c}$$

from which it follows that $u_s = u_m + u_{\mathrm{diff},s}$, $v_s = v_m + v_{\mathrm{diff},s}$ and $v_s = u_s$. Use of the species velocities can cause confusion, however, and in the main text the analysis is couched completely in terms of fluxes. Velocities are only used where necessary in Appendices 1 and 2.

Many authors (e.g., [6]) use a non-standard formalism in which G_s and J_s are split into what are termed *forced* and *diffusive* fluxes. Although these are not defined precisely, the forced fluxes seem to be those associated with a pressure gradient while the diffusive fluxes represent the remainder. This approach is invariably problematic because the diffusive fluxes no longer sum to zero. Also, the physics becomes obscured and ambiguities, not easy to resolve, arise concerning a so-called *viscous flow* term. Non-standard flux decomposition is therefore not to be recommended (see also Kerkhof [9] on this topic).

4. Continuum flow in a straight pore

The analysis starts by considering multi-component flow in a single pore. Single-component, fully-developed, laminar viscous flow in a straight capillary tube of radius R at the continuum limit of very small Knudsen number is known as Poiseuille flow and the solution for the mass flowrate in terms of the applied pressure gradient has been known for centuries. However, when the fluid is a multi-component mixture of ideal gases diffusing longitudinally the problem is much more complicated.

An analysis for the special case of the equimolar counter-diffusion of a binary mixture was first given by Kramers and Kistemaker [12] and this was extended to more general multi-component flows by Jackson, see Chapter 4 of [8]. Given that binary Poiseuille flow is one of the most fundamental examples of convective-diffusive flow, it is surprising that these works are seldom

quoted. Indeed, the usual textbook analysis of equimolar diffusion ignores the effect of the tube walls completely and thereby arrives at a result which is at variance with a substantial number of experimental studies leading all the way back to the 19th century work of Graham, see Chapter 6 of [8]. Graham's empirical *law of diffusion* is often mentioned in textbook introductions but the theory of later chapters seemingly contradicts it, usually without explanation. The problem can be traced to the wall boundary condition.

4.1. The wall boundary condition

In single-component viscous flow the condition of zero velocity applied at solid boundaries is a reliable, well-established approximation. Indeed, so strongly is the no-slip condition embedded in the fluid dynamicist's psyche that even in binary or multi-component flow, the mass-mean flow velocity at a wall is usually set to zero without further consideration, for example as in Mills [13]. For capillary flow, however, this assumption is incorrect and may generate serious errors if the convective contributions are small and there is a large disparity in the molar masses of the gas components.

Kramers and Kistemaker [12] were the first to examine the wall boundary condition in detail. As shown in Fig. 1, they considered an infinite expanse of a constant pressure binary gas mixture adjacent to a solid wall. Using elementary kinetic theory, they predicted that, in the presence of a concentration gradient parallel to the wall, the mixture would flow along the wall with non-zero mass-mean velocity. They called this phenomenon *diffusion slip*.

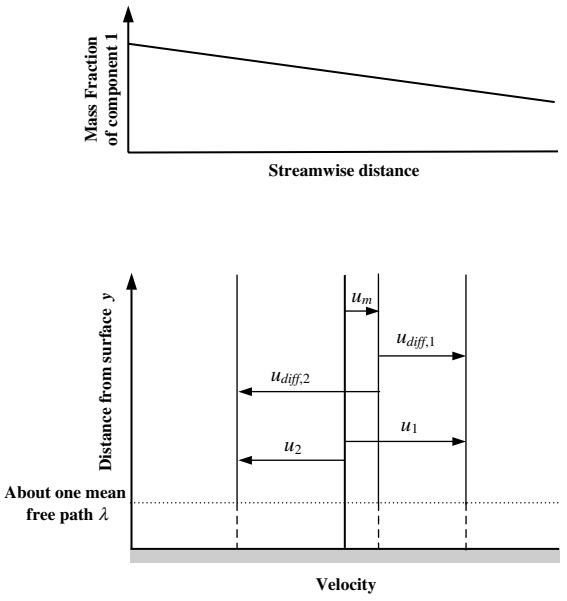

Fig. 1. Illustrating mass diffusion slip for a binary mixture ($M_1 < M_2$) near a solid surface in the presence of a streamwise mass fraction gradient. For $y < \lambda$ the molecular velocity distribution functions of the gas species are non-Maxwellian and the dashed lines represent extrapolations to the wall of the (constant) values in the bulk.

Diffusion slip is different from *viscous* slip which is a well-known effect occurring in tube-flow when the pressure is such that the molecular mean free path λ is a significant fraction of the tube radius ($Kn = \lambda/2R > 0.1$). The slip (or extrapolated) velocity at the wall is then proportional to the velocity gradient near the wall. Viscous slip vanishes at the continuum limit and this is, of course, the origin of the no-slip boundary condition of continuum fluid mechanics.

In multi-component tube-flow diffusion slip is important at all Knudsen numbers and exists even when the streamwise pressure gradient is zero. Viscous slip is important only when $Kn > 0.1$ and there is an applied pressure gradient resulting in a parabolic velocity profile. The combined effect of the two phenomena was analysed by Jackson [8] by amalgamating the Kramers and Kistemaker theory with viscous slip theory as described by Kennard [14].

Jackson's result was obtained using the simplest possible kinetic model for momentum transport in gas mixtures. However, it has been known since the time of Maxwell that this model is not successful at predicting the viscosity of mixtures if the component gases have diverse molar masses. An improved theory was developed by Sutherland [15]. This embodied the correct physics but required an empirical adjustment to give agreement with the experimental measurements of the time. Later, Sutherland's theory formed the basis of the viscosity prediction method of Wilke [16] which, according to Poling et al. [17], is still considered to be one of the best available for gas mixtures. An outline of Sutherland's theory is given in Appendix 1.

It is straightforward to modify Jackson's theory to include Sutherland's momentum transport model and the details are given in Appendix 1. Surprisingly, the expression for the diffusion slip velocity in the continuum limit turns out to be unaltered from Jackson's result (which itself is just a multi-component version of the Kramers and Kistemaker expression). In the viscous slip-flow regime, Sutherland's model does indeed make itself felt but this result is not actually required for the present theory. As noted in Section 3 above, it is generally more convenient to work in terms of fluxes rather than velocities and the results of Appendix 1 are therefore converted to this form. Thus, *for continuum flow only*, the mass-mean and molar-mean diffusion slip *fluxes* at the tube wall, $G(R)$ and $J(R)$, are given by,

$$G(R) = -\frac{\sum M_s^{-1/2} G_{\mathrm{diff},s}}{\sum Y_s M_s^{-1/2}} \tag{5a}$$

$$J(R) = -\frac{\sum M_s^{1/2} J_{\mathrm{diff},s}}{\sum X_s M_s^{1/2}} \tag{5b}$$

where it has been assumed in the derivation that the diffuse reflection coefficients for all gas molecules impacting the wall are equal. $G_{\mathrm{diff},s}$ and $J_{\mathrm{diff},s}$ are the mass and molar diffusion fluxes which, *under the assumptions of the present theory*, are constant over the tube cross-section (see Section 4.2 below for justification). For a binary mixture, Eq. (5a) written in terms of velocities is identical to Eq. (9) of Kramers and Kistemaker [12].

A near-wall kinetic theory analysis can also be found in the MPTM derivation by Schneider [6] but this paper is difficult to interpret because of the non-standard decomposition into forced and diffusive fluxes mentioned previously. Schneider's theory certainly allows for viscous slip but his Eq. (18) shows that, for zero pressure gradient, all component velocities at the wall vanish. This seems to imply that diffusion slip has not been included.

Clearly, care is required in dealing with the wall condition and the comparatively crude analysis leading to Eq. (5) is itself open to criticism. Over the years, there have been attempts to improve on the situation through direct molecular dynamics simulations, e.g., Mo and Rosenberger [18], and by solving model versions of the Boltzmann equation in the near-wall region, e.g., Kanki et al. [19], Takata et al. [20] and Sharipov and Kalempa [21]. Most of this work is mathematically complex and difficult to assess, and sometimes involves restrictive modelling assumptions. Nevertheless, it is worth noting the 'exact' solution of the BGK equation by Lang and Loyalka [22] which might be of value for testing the accuracy of the simple models. In summary, the more complex theories indicate that the diffusion slip flux probably depends on the sizes as well as the masses of the molecules involved, although the form of this dependence has not been expressed explicitly. A proper assessment requires a major exercise which is outside both the scope and spirit of the present paper.

4.2. The Stefan–Maxwell equations

In continuum flow, the component fluxes are related to the mole or mass fraction gradients by the Stefan–Maxwell equations. Kinetic theory provides a rigorous derivation of these equations for a uniform velocity field [23] but the question arises as to whether a non-uniform velocity field resulting in cross-stream momentum transfer (as in Poiseuille flow) also affects the diffusive fluxes. This is an important point because the BFM theory of Kerkhof [9] and the VPM theories of Kerkhof et al. [10] all start from modified forms of the Stefan–Maxwell equations which include extra shear stress related terms which affect the diffusive fluxes. As these modifications add considerably to the complexity of the analysis and also tend to obscure the underlying physics, it is important to assess the significance of the corrections. The problem is considered in Appendix 2 where a kinetic theory derivation of the Stefan–Maxwell equations is presented showing exactly how the extra shear stress terms advocated by Kerkhof et al. arise. It is concluded that, given the uncertainty in modelling the collisional momentum transfer terms in the presence of velocity gradients, inclusion of the Kerkhof terms cannot really be justified at the present time. Furthermore, as noted above, neglect of these terms has the substantial advantage that the resulting analysis is far simpler and more physically informative. To see this, the present analysis should be contrasted with that of Kerkhof et al. [10].

Accordingly, the mass and molar forms of the basic Stefan–Maxwell equations (written in terms of the total component fluxes rather than the diffusive fluxes) are,

$$\rho \frac{\mathrm{d}Y_s}{\mathrm{d}\xi} = \sum_r \left[\frac{Y_s G_r}{(D_\mathrm{B})_{rs}} - \frac{Y_r G_s}{(D_\mathrm{B})_{sr}} \right] \tag{6a}$$

$$c \frac{\mathrm{d}X_s}{\mathrm{d}\xi} = \sum_r \left[\frac{X_s J_r}{(D_\mathrm{B})_{rs}} - \frac{X_r J_s}{(D_\mathrm{B})_{sr}} \right] \tag{6b}$$

where $(D_\mathrm{B})_{rs} = (D_\mathrm{B})_{sr}$ is the binary diffusion coefficient for a mixture of gas species r and s. The Chapman–Enskog expression for $(D_\mathrm{B})_{sr}$ is

$$(D_\mathrm{B})_{sr} = \frac{3}{16 n \sigma_{sr}^2 \Omega_{sr}} \left[\frac{2R_\mathrm{g} T}{\pi} \left(\frac{1}{M_s} + \frac{1}{M_r} \right) \right]^{1/2} \tag{7}$$

where n is the number density of molecules, σ_{sr} is the collision diameter of the s–r molecule pair and Ω_{sr} is a factor of order unity which depends on the intermolecular force.

There are N equations of the form of Eq. (6) (one for each component) but only $N-1$ are independent because the mole or mass fractions sum to unity. Sometimes, contributions from thermal and pressure diffusion (see Appendix 2) are also included as in Mason and Malinauskas [4], but the gain in accuracy is questionable and such terms are best neglected unless there are good reasons for their inclusion.

More generally, the Stefan–Maxwell equations are a set of vector equations of which Eq. (6) represent the streamwise components only. Consideration of the radial components in the context of Poiseuille flow shows that Y_s and X_s are independent of radius and only vary with ξ. This justifies the use of the total derivatives $\mathrm{d}Y_s/\mathrm{d}\xi$ and $\mathrm{d}X_s/\mathrm{d}\xi$ in Eq. (6). Also, because the left hand sides of Eq. (6) are independent of radius, so too are the right hand sides and, with Eq. (3), it then follows that the diffusive fluxes $G_{\mathrm{diff},s}$ and $J_{\mathrm{diff},s}$ are individually independent of radius. This result was used in the derivation of Eq. (5).

Although $G_{\mathrm{diff},s}$ and $J_{\mathrm{diff},s}$ are independent of radius r, the same is not true of the fluxes G_s, J_s, G and J. As shown in Section 4.3 below, when the pressure gradient

is non-zero, these actually vary parabolically across the tube. Cross-sectional or tube-averaged values of G_s and J_s (denoted by overbars) can therefore be defined by the relations,

$$\pi R^2 \overline{G}_s = \int_0^R 2\pi r\, G_s(r)\,\mathrm{d}r \quad \pi R^2 \overline{G} = \int_0^R 2\pi r G(r)\,\mathrm{d}r \tag{8a}$$

$$\pi R^2 \overline{J}_s = \int_0^R 2\pi r J_s(r)\,\mathrm{d}r \quad \pi R^2 \overline{J} = \int_0^R 2\pi r J(r)\,\mathrm{d}r \tag{8b}$$

Integration of Eq. (6) from $r = 0$ to $r = R$ then gives,

$$\rho\left(\frac{\mathrm{d}Y_s}{\mathrm{d}\xi}\right)_{\mathrm{C}} = \sum_r \left[\frac{Y_s\overline{G}_r}{(D_{\mathrm{B}})_{rs}} - \frac{Y_r\overline{G}_s}{(D_{\mathrm{B}})_{sr}}\right] \tag{9a}$$

$$c\left(\frac{\mathrm{d}X_s}{\mathrm{d}\xi}\right)_{\mathrm{C}} = \sum_r \left[\frac{X_s\overline{J}_r}{(D_{\mathrm{B}})_{rs}} - \frac{X_r\overline{J}_s}{(D_{\mathrm{B}})_{sr}}\right] \tag{9b}$$

The subscript C indicates that the equations are only valid in the continuum limit $Kn \to 0$.

For Poiseuille flow, it is evident that the Stefan–Maxwell equations take the same form whether written in terms of the local fluxes at a given radius, as in Eq. (6), or as tube-averaged values, as in Eq. (9). This is not the case if, as in Kerkhof et al. [10], the species *shear-stress-difference* term (the term in large square brackets in Eq. (A2.6) in Appendix 2) is included. The subsequent analysis is then much more complicated and any improvement in accuracy is obtained at a high price.

4.3. The pressure gradient

Application of the force–momentum principle to a cylindrical control volume of radius r and length $\delta\xi$ gives,

$$2\pi r\left(\mu\frac{\partial(G/\rho)}{\partial r}\right) = \pi r^2\frac{\partial p}{\partial \xi} + \frac{\partial}{\partial \xi}\left(\int_0^r 2\pi r'\frac{G^2}{\rho}\,dr'\right) \tag{10}$$

where G depends on the radius but p and ρ are functions of ξ only. The final term represents the streamwise variation of momentum flux and only occurs in multi-component flow because diffusion causes the mixture density to vary along the tube. Dullien and Scott [24] have provided an interesting analysis of the effect of this term when the pressure gradient is zero. Their findings show that, *specifically for fully-developed flow in long capillaries*, the term can be neglected.

Accordingly, integration with respect to r of Eq. (10) without the final term gives

$$G(r) = G(R) + \rho\left(\frac{R^2 - r^2}{4\mu}\right)\left(-\frac{\mathrm{d}p}{\mathrm{d}\xi}\right) \tag{11}$$

which shows that the mass-mean profile is parabolic (as in single-component flow) but is generally non-zero at the wall. From Eq. (8a) the total tube-averaged mass flux is

$$\overline{G} = G(R) + \frac{\rho R^2}{8\mu}\left(-\frac{\mathrm{d}p}{\mathrm{d}\xi}\right) \tag{12}$$

From Eq. (3a) the component fluxes are given by $G_s(r) = Y_s G(r) + G_{\mathrm{diff},s}$ which shows that G_s also varies parabolically with r. It then follows from Eq. (8a) that the tube-averaged values are related by $\overline{G}_s = Y_s\overline{G} + G_{\mathrm{diff},s}$ (i.e., exactly the same form as the local relationship).

The simplicity of the above analysis is a result of working with a mass formulation throughout and should be contrasted with the relentless complexity of the hybrid mass/molar derivation by Jackson in Chapter 4 of [8]. Transformation to the molar form is easily achieved by noting that $G_s = M_s J_s$ and hence $\overline{G}_s = M_s\overline{J}_s$. In general, of course, $\overline{G} \neq M\overline{J}$ (where M is the mean molar mass).

Substituting from Eq. (5a) for $G(R)$ in Eq. (12), and using $\overline{G}_s = Y_s\overline{G} + G_{\mathrm{diff},s}$ to eliminate $G_{\mathrm{diff},s}$ gives the desired expression for the pressure gradient, given here in both mass and molar forms:

$$\left(\frac{\mathrm{d}p}{\mathrm{d}\xi}\right)_{\mathrm{C}} = -A_{\mathrm{C}}\sum_s M_s^{-1/2}\overline{G}_s \quad A_{\mathrm{C}} = \frac{8\mu}{\rho R^2\sum_s Y_s M_s^{-1/2}} \tag{13a}$$

$$\left(\frac{\mathrm{d}p}{\mathrm{d}\xi}\right)_{\mathrm{C}} = -A_{\mathrm{C}}\sum_s M_s^{1/2}\overline{J}_s \quad A_{\mathrm{C}} = \frac{8\mu}{cR^2\sum_s X_s M_s^{1/2}} \tag{13b}$$

With properly specified tube-end boundary conditions (various allowable combinations of concentrations and fluxes), there will be N unknowns and these will be fully-specified by Eq. (13a) or (13b) and the $N-1$ independent versions of Eq. (9a) or (9b).

4.4. Continuum flow of a binary mixture

It is interesting to examine the reduction of Eqs. (9) and (13) for the case of a binary mixture. For the case of zero pressure gradient, $\mathrm{d}p/\mathrm{d}\xi = 0$, G and J are constant over the tube cross-section and Eq. (13b) reduces to the relation

$$\frac{\overline{J}_1}{\overline{J}_2} = -\sqrt{\frac{M_2}{M_1}} \tag{14}$$

which is known as *Graham's law of diffusion*. This was deduced by Graham around the middle of the 19th century from his experiments on gas diffusion and has been confirmed with reasonable accuracy by the later experimental work of Hoogschagen [25], Scott and Cox [26], Rothwell [5] and others. Eq. (14) is a direct result of introducing Eq. (5a) for the wall slip flux $G(R)$ into Eq. (12). If $G(R)$ were set equal to zero, then Eq. (14) would be replaced by $\overline{J}_1/\overline{J}_2 = -M_2/M_1$ which is not in agreement with experimental measurements. Fig. 2a provides an illustration of Eq. (14) for the constant pressure counter-diffusion of air and hydrogen.

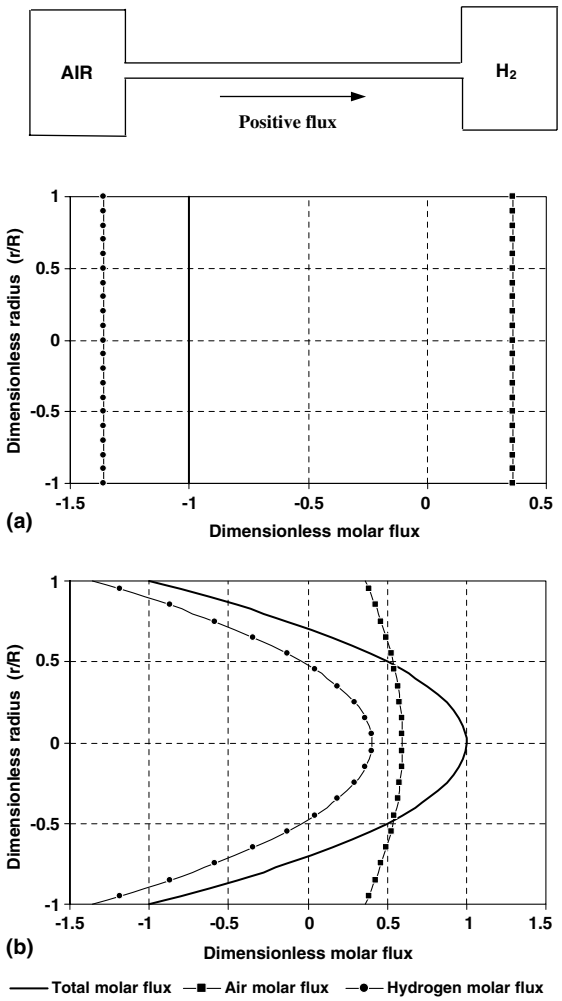

Fig. 2. Counter-diffusion of air and hydrogen in a tube. Flux profiles for: (a) zero pressure gradient, (b) equimolar diffusion. All fluxes non-dimensionalised by the molar slip flux. In (a) $\overline{J}_{H_2}/\overline{J}_{Air} = -\sqrt{M_{Air}/M_{H_2}} = -3.78$.

Another simple binary flow of interest is tube-averaged equimolar counter-diffusion. For this situation, Eq. (9b) reduce to

$$\overline{J}_1 = -\overline{J}_2 = -cD_{12}\frac{\mathrm{d}X_1}{\mathrm{d}\xi} \tag{15}$$

Substituting into Eq. (13b) and integrating along the tube gives the overall pressure difference Δp. Assuming pure species 1 at one end, pure species 2 at the other, and constant μ and D_{12}, Δp is easily shown to be given by the Kramers and Kistemaker result,

$$\Delta p = \frac{4\mu D_{12}}{R^2}\ln\left(\frac{M_2}{M_1}\right) \tag{16}$$

which is half the value obtained if diffusion slip is neglected. Kramers and Kistemaker also made experimental measurements of Δp for the equimolar counter-diffusion of hydrogen and air and found agreement with Eq. (16) to within about 30%. The discrepancy may have been due, in part, to the fact that the viscosity μ was not constant along the tube because of the variation in gas mixture composition.

As equimolar counter-diffusion requires a pressure gradient, the fluxes vary parabolically across the tube as shown in Fig. 2b for the case of air and hydrogen. The calculations were performed by the method described in Section 7.3 below. It is interesting to note that although the H_2 flux is negative near the walls, it is actually positive in the central region where the negative diffusive flux is outstripped by the positive convective flux. Such behaviour, and the importance of specifying tube-averaged values in certain theoretical work does not seem to be generally appreciated.

In summary, it can be stated that the available experimental evidence provides quite good support for the theory of diffusion slip in continuum flow.

5. Free-molecule flow in a straight tube

5.1. Kinetic theory solution

Free-molecule flow occurs when the species mean free paths are much greater than the tube diameter ($Kn \gg 1$) so that wall collisions dominate over inter-molecular collisions and each gas species behaves independently. Using kinetic theory, an equation can be derived relating the s-species total molar flux J_s to the molar concentration gradient $\mathrm{d}c_s/\mathrm{d}\xi$, see Kennard [14]. Assuming that the tube length is much greater than its diameter and the flow is isothermal, the result is

$$\overline{J}_s = -\frac{(2-f_s)}{f_s}\frac{2R\bar{w}_s}{3}\frac{\mathrm{d}c_s}{\mathrm{d}s} = -(D_K)_s\frac{\mathrm{d}c_s}{\mathrm{d}\xi} \tag{17}$$

where R is the tube radius and f_s and $\bar{w}_s$ are, respectively, the diffuse reflection coefficient and mean molecular speed of species-s molecules. It should be noted that J_s is not quite uniform over the tube cross-section and Eq. (17) gives the tube-averaged value. $(D_K)_s$ is often referred to as the *Knudsen diffusion coefficient* but this is misleading because Eq. (17) is a relation for the total, rather then the diffusive, flux. From Eq. (A1.2) in Appendix 1

$$(D_K)_s = \frac{(2-f_s)}{f_s}\frac{2R}{3}\left(\frac{8R_gT}{\pi M_s}\right)^{1/2} \tag{18}$$

and it is important to note that $(D_K)_s$ is inversely proportional to $M_s^{1/2}$.

Schneider [6] expanded Eq. (17) into a *diffusion flux* involving the mole fraction gradient and a *forced flux* involving the pressure gradient. This is analytically

correct but the diffusion fluxes do not sum to zero. If, however, the procedure of Section 3 is applied, as in Rothwell [5], it is found that the true diffusion coefficients depend on the mole fractions and flux ratios, which is clearly undesirable. It is therefore best to work with Eq. (17) as it stands.

For each of the N species, there is one equation of the form of Eq. (17). With properly specified tube-end boundary conditions, these are sufficient to solve for the N unknowns. However, to obtain equations for transitional Knudsen numbers, it is necessary to interpolate between the continuum and free-molecule limits. Eqs. (9) and (13) for continuum flow and Eq. (17) for free-molecule flow have different forms and this creates an interpolation problem which is awkward to solve cleanly and elegantly.

The way forward is to note that $c_s = X_s p/R_g T$ and to expand Eq. (17) to give

$$\frac{R_g T}{(D_K)_s}\overline{J}_s = -\left(p\frac{\mathrm{d}X_s}{\mathrm{d}\xi} + X_s\frac{\mathrm{d}p}{\mathrm{d}\xi}\right) \tag{19}$$

This is similar to Schneider [6] but the intent is different. Summing over all components gives, in mass and molar forms, the following equations for the pressure gradient (for $f_s = 1$),

$$\left(\frac{\mathrm{d}p}{\mathrm{d}\xi}\right)_K = -A_K\sum_s M_s^{-1/2}\overline{G}_s$$

$$A_K = \frac{R_g T}{(D_K)_s M_s^{1/2}} = \frac{3}{4R}\left(\frac{\pi R_g T}{2}\right)^{1/2} \tag{20a}$$

$$\left(\frac{\mathrm{d}p}{\mathrm{d}\xi}\right)_K = -A_K\sum_s M_s^{1/2}\overline{J}_s$$

$$A_K = \frac{R_g T}{(D_K)_s M_s^{1/2}} = \frac{3}{4R}\left(\frac{\pi R_g T}{2}\right)^{1/2} \tag{20b}$$

The subscript K indicates that Eq. (20) are only valid in the limit $Kn \to \infty$. It will be noted that neither the case $\overline{J} = 0$ nor $\overline{G} = 0$ corresponds, in general, to zero pressure gradient in free-molecule flow. Substituting Eq. (20b) into Eq. (19), using $p = cR_g T$ and rearranging gives

$$c\frac{\mathrm{d}X_s}{\mathrm{d}\xi} = X_s\sum_r\frac{\overline{J}_r}{(D_K)_r} - \frac{\overline{J}_s}{(D_K)_s} \tag{21}$$

which may be written more informatively (together with the mass version) as:

$$\rho\left(\frac{\mathrm{d}Y_s}{\mathrm{d}\xi}\right)_K = \sum_r\left[\frac{Y_s\overline{G}_r}{(D_K)_r} - \frac{Y_r\overline{G}_s}{(D_K)_s}\right] \tag{22a}$$

$$c\left(\frac{\mathrm{d}X_s}{\mathrm{d}\xi}\right)_K = \sum_r\left[\frac{X_s\overline{J}_r}{(D_K)_r} - \frac{X_r\overline{J}_s}{(D_K)_s}\right] \tag{22b}$$

Eqs. (20) and (22) have exactly the same form as Eqs. (13) and (9) for continuum flow.

5.2. Free-molecule flow of a binary mixture

For a binary mixture with zero pressure gradient, Eq. (20b) reduces to

$$\frac{\overline{J}_1}{\overline{J}_2} = -\sqrt{\frac{M_2}{M_1}} \tag{23}$$

which is often referred to as *Graham's law of effusion* although it was actually Knudsen who established its validity. Given that Graham's experiments were exclusively in the continuum regime, it seems only fair that the 'law' should be renamed to give Knudsen the credit.

Eq. (23) is the same as Eq. (14), although the theory leading to each is quite different. Early papers expressed the hope that measurements of $\overline{J}_1/\overline{J}_2$ in a constant pressure counter-diffusion test on a sample of porous material would yield a value of the mean pore radius but this is clearly not possible given the same square-root relationship at both limits.

6. Flow at arbitrary Knudsen number

No simple theory exists for flow at transitional Knudsen numbers. The problem, which really requires solution of the species Boltzmann equations, is notoriously difficult and all simple forms found in the literature are actually based on mathematical interpolation rather than physical principles. However, even the interpolation procedures are often unclear because of the asymmetry of the continuum and free-molecule equations. Here, the equations have been deliberately manipulated so that Eqs. (9) and (22) for the continuum and free-molecule mass or mole fraction gradients, and Eqs. (13) and (20) for the pressure gradients, have a high degree of symmetry. Choosing a suitable interpolation method is then much more obvious.

6.1. Interpolation for the mass/mole fraction gradients

A comparison of Eqs. (9) and (22) shows that the basic requirement of any interpolation procedure is the specification of a coefficient $(D_A)_{sr}$ for arbitrary Knudsen numbers Kn such that $(D_A)_{sr} \to (D_B)_{sr}$ as $Kn \to 0$ and $(D_A)_{sr} \to (D_K)_r$ as $Kn \to \infty$.

The definition of the Knudsen number is to a certain extent arbitrary, although it obviously has to represent the ratio of a mean free path to the tube radius. If a mean free path λ_{sr} is *defined* by the kinetic-based expression $\lambda_{sr} = (\sqrt{2}\pi\, n\, \sigma_{sr}^2)^{-1}$, then $(D_B)_{sr}$ from Eq. (7) and $(D_K)_s$ from Eq. (18) with $f_s = 1$ are related by

$$\frac{(D_B)_{sr}}{(D_K)_s} = \frac{9\pi}{16\sqrt{2}\Omega_{sr}}\left(1 + \frac{M_s}{M_r}\right)^{1/2} Kn_{sr} = C_{sr}Kn_{sr} \tag{24}$$

where $Kn_{sr} = \lambda_{sr}/R$ and the coefficient C_{sr} is of order unity. In practice, it is more useful to absorb C_{sr} into

the definition of the Knudsen number. Accordingly, a *diffusion* Knudsen number is defined by the relation, $(Kn_D)_{sr} = (D_B)_{sr}/(D_K)_s$.

The simplest interpolation formula fulfilling the basic requirement is

$$(D_A)_{sr} = \frac{(D_B)_{sr}}{1 + (Kn_D)_{sr}} \tag{25}$$

which is often expressed in the Bosanquet form, see Pollard and Present [27].

$$\frac{1}{(D_A)_{sr}} = \frac{1}{(D_B)_{sr}} + \frac{1}{(D_K)_s} \tag{26}$$

It must be emphasised that Eq. (26) has no physical basis and about the only evidence to suggest that it might provide accurate interpolation is the good agreement recorded by Pollard and Present with their mean free path theory of the self-diffusion coefficient.

The interpolated forms of Eqs. (9) and (22) for use at any Knudsen number are thus:

$$\rho \frac{\mathrm{d}Y_s}{\mathrm{d}\xi} = \sum_r \left[\frac{Y_s \overline{G}_r}{(D_A)_{rs}} - \frac{Y_r \overline{G}_s}{(D_A)_{sr}} \right] \tag{27a}$$

$$c \frac{\mathrm{d}X_s}{\mathrm{d}\xi} = \sum_r \left[\frac{X_s \overline{J}_r}{(D_A)_{rs}} - \frac{X_r \overline{J}_s}{(D_A)_{sr}} \right] \tag{27b}$$

It should be noted that $(D_A)_{sr} \neq (D_A)_{rs}$ except when $M_s = M_r$.

6.2. Interpolation for the pressure gradient

Specifying a *bulk* or *viscous* flow term at arbitrary Knudsen number has always caused problems. Thus, Kerkhof [9], with inspired phraseology, accuses the authors of the DGM of *trying to talk an extra viscous term into an equation which already contains the same term*! It is a particular feature of the present work that this problem does not arise because the deliberate symmetry of Eqs. (13) and (20) can be exploited to provide an obvious method of interpolation for the pressure gradient at any Knudsen number.

As before, a mean free path λ is defined by a kinetic-based expression, in this case $\mu = (\rho\ \bar{w}\ \lambda)/2$, where μ is the mixture viscosity and $\bar{w}$ is a mean molecular speed defined by Eq. (A1.2) with M_s replaced by the mean molar mass $M = \sum X_s M_s$. The ratio of the coefficients A_C and A_K in Eqs. (13) and (20) can then be written

$$\frac{A_C}{A_K} = \frac{64}{3\pi} \frac{\left(\sum X_s M_s\right)^{1/2}}{\left(\sum X_s M_s^{1/2}\right)} \frac{\lambda}{R} = C\,Kn \tag{28}$$

where $Kn = \lambda/R$ is another Knudsen number and C is a constant of magnitude 5–10. This somewhat larger constant can be absorbed into the definition of a *pressure* Knudsen number, $Kn_P = A_C/A_K$.

The simplest interpolation formula giving the correct limiting behaviour is, therefore,

$$A_A = \frac{A_C}{1 + Kn_P} \tag{29}$$

or, alternatively,

$$\frac{1}{A_A} = \frac{1}{A_C} + \frac{1}{A_K} \tag{30}$$

The expressions for the pressure gradient at arbitrary Knudsen number are then

$$\frac{\mathrm{d}p}{\mathrm{d}\xi} = -A_A \sum_s M_s^{-1/2} \overline{G}_s \tag{31a}$$

$$\frac{\mathrm{d}p}{\mathrm{d}\xi} = -A_A \sum_s M_s^{1/2} \overline{J}_s \tag{31b}$$

With the appropriate tube-end boundary conditions, Eqs. (27) with (26), and (31) with (30) completely specify multi-component flow in a straight tube at arbitrary Knudsen number. It is worth re-iterating that the interpolation prescriptions defined by Eqs. (26) and (30) are arbitrary and that there are no a priori theoretical reasons for supposing that they provide a good representation at transitional Knudsen numbers.

7. Flow in porous solids

7.1. The governing equations

The analysis so far has been concerned with flow in straight capillary tubes and the extension to porous solids is not straightforward. The simplest approach is to introduce two parameters, the *porosity* ε and *tortuosity* τ, which take account, respectively, of the connected void space in the medium and the extended length of the pores due to their circuitous paths. The porosity can usually be measured directly but the tortuosity is treated as an empirical parameter to be obtained indirectly from certain types of flow experiment and the success of the model depends largely on whether the tortuosity remains constant over the required range of interest.

Only the simplest structures (which, by their assumed uniformity are plainly not representative of real porous material) can be modelled rigorously. Epstein [28] discusses the correct implementation of ε and τ into the equations and his approach is followed here. If distance ξ is measured along a pore and z normal to the porous slab surface, then $\tau = \mathrm{d}\xi/\mathrm{d}z$ and is assumed constant through the material. The pore-averaged fluxes (denoted by overbars) are then related to the fluxes crossing unit area of slab (denoted by *tildes*) according to

$$\widetilde{G}_s = \frac{\varepsilon}{\tau}\overline{G}_s \quad \widetilde{J}_s = \frac{\varepsilon}{\tau}\overline{J}_s \tag{32}$$

Noting that $\mathrm{d}/\mathrm{d}\xi$ transforms as $(1/\tau)\mathrm{d}/\mathrm{d}z$, Eqs. (27) and (31) become, in the mass formulation,

$$\frac{\rho\varepsilon}{\tau^2}\frac{\mathrm{d}Y_s}{\mathrm{d}z} = \sum_r \left[\frac{Y_s\widetilde{G}_r}{(D_\mathrm{A})_{rs}} - \frac{Y_r\widetilde{G}_s}{(D_\mathrm{A})_{sr}}\right] \tag{33a}$$

$$\frac{\varepsilon}{\tau^2}\frac{\mathrm{d}p}{\mathrm{d}z} = -A_\mathrm{A}\sum_s M_s^{-1/2}\widetilde{G}_s \tag{33b}$$

and in the molar formulation,

$$\frac{c\varepsilon}{\tau^2}\frac{\mathrm{d}X_s}{\mathrm{d}z} = \sum_r \left[\frac{X_s\widetilde{J}_r}{(D_\mathrm{A})_{rs}} - \frac{X_r\widetilde{J}_s}{(D_\mathrm{A})_{sr}}\right] \tag{34a}$$

$$\frac{\varepsilon}{\tau^2}\frac{\mathrm{d}p}{\mathrm{d}z} = -A_\mathrm{A}\sum_s M_s^{1/2}\widetilde{J}_s \tag{34b}$$

Eqs. (33) or (34) represent the complete set of governing equations for the convective-diffusive flow in a porous medium at arbitrary Knudsen number. Compared with other forms found in the literature, their simplicity and compactness is striking. The flow coefficients D_A are given by Eq. (26) with D_B from Eq. (7) (or an appropriate empirical expression) and D_K from Eq. (18). The pressure gradient coefficient A_A is given by Eq. (30) with A_C from Eq. (13) and A_K from Eq. (20). The pore radius R which appears in the expressions for A_C, A_K and D_K is interpreted as a mean value to be determined experimentally. The parameters ε and τ enter in the combination ε/τ^2 (often derived incorrectly as ε/τ) and can be treated as a single scaling parameter if desired. Alternatively, it is often informative to separate the effects of ε and τ because ε can usually be measured quite precisely.

By combining the (a) and (b) forms of Eqs. (33) or (34) in various ways, it is possible to make comparisons with other models in the literature, particularly the DGM, MPTM and BFM. This is an instructive exercise but will not be carried further here as the main objective is to focus on the attributes of the CPIM formulation.

7.2. Interpretation of the CPIM equations

In order to apply the CPIM theory, it is necessary to obtain values of R and ε/τ^2 for the porous solid of interest. The same is true for all the other theories, although the empirical parameters may appear in different guises depending on the assumptions of the theory and method of presentation of the equations. In order to obtain information, it has been traditional to perform experiments to measure the *effective diffusivities* of the gases and the *permeability* of the medium, and most studies start from such measurements.

The term *effective diffusivity* refers to a modified form of the flow coefficient D_A in which the factor ε/τ^2 has been absorbed. Concealing the physical origin of ε/τ^2 in this way is not a good strategy, however, particularly as the factor also appears in the pressure gradient equation.

Permeability is a measure of the resistance to the flow of a single gas component through the porous sample. Thus, the permeability K_s of gas species-s is defined by

$$\widetilde{J}_s = -\frac{K_s}{R_\mathrm{g}T}\frac{\mathrm{d}p}{\mathrm{d}z} \tag{35}$$

all other species being absent. For the CPIM, K_s is given by rearranging Eq. (34b) and introducing Eq. (13b) for A_C and Eq. (20b) for A_K with the result

$$K_s = \frac{R_\mathrm{g}T}{\sqrt{M_s}}\left(\frac{1}{A_\mathrm{C}} + \frac{1}{A_K}\right)\frac{\varepsilon}{\tau^2} = \left[\frac{Rp}{8\mu} + \frac{2}{3}\left(\frac{8R_\mathrm{g}T}{\pi M_s}\right)^{1/2}\right]\frac{R\varepsilon}{\tau^2} \tag{36}$$

Permeability measurements are always extrapolated to zero pressure and Eq. (36) shows that, for the CPIM, this provides a measure of the combined parameter $R\varepsilon/\tau^2$. The permeability expressions for the DGM and MPTM are similar, thus confirming that *permeability measurements on their own cannot separate the fundamental parameters characterising the porous medium*.

There is no need, however, to set about the analysis in this way and the special form of the CPIM equations suggests a completely different approach and interpretation which will now be described. Working with the molar formulation, Eq. (34), it can be seen that ε/τ^2 can be eliminated by dividing Eq. (34a) by (34b) to give

$$-cA_\mathrm{A}\sum_s M_s^{1/2}\widetilde{J}_s\frac{\mathrm{d}X_s}{\mathrm{d}p} = \sum_r\left[\frac{X_s\widetilde{J}_r}{(D_\mathrm{A})_{rs}} - \frac{X_r\widetilde{J}_s}{(D_\mathrm{A})_{sr}}\right] \tag{37}$$

and there are $N-1$ independent equations of this form.

Consider the common situation when p and the X_s values on each side of the porous sample are given (i.e., at $z=0$ and $z=L$), and the N fluxes $\widetilde{J}_s$ are unknown. In principle, Eq. (37) can be integrated across the sample to give $N-1$ independent equations relating the overall changes $\Delta p = p(L) - p(0)$ and $\Delta X_s = X_s(L) - X_s\,(0)$. Clearly these equations are insufficient to solve for the N fluxes *but they are sufficient to solve for the $N-1$ flux ratios* (i.e., $\widetilde{J}_1/\widetilde{J}_2$ etc).

The only empirical parameter in Eq. (37) is the mean pore radius R (which appears in the coefficients A_A and D_A). The CPIM formulation has therefore allowed the remarkable prediction that, for fixed pressure and mole fraction boundary conditions, the flux ratios are independent of the porosity and tortuosity and only depend on the mean pore radius. In other words, apart from the mean pore radius, the structure of the material plays no part in deciding the flux ratios: for the same boundary conditions, a straight capillary of radius R should behave in the same way as a porous solid with mean pore radius R.

Of course, the absolute flux magnitudes do depend on ε and τ, and integration of Eqs. (33a) or (34b) can be used to calculate the chosen reference flux. This is

the only point when ε/τ^2 and the spatial co-ordinate z enter the calculation and suggests an obvious physical interpretation for ε/τ^2 as a spatial scaling factor. Indeed, by defining a scaled length variable $z' = z\tau^2/\varepsilon$, Eqs. (33) and (34) become identical to Eqs. (27) and (31) for the flow in straight capillaries. This is a much better physical interpretation of ε/τ^2 than the usual interpretation in terms of modified gas diffusivities and permeabilities.

7.3. Comparison with experimental measurements for binary flow

The ideas of the previous section become much clearer in the special context of binary diffusion which also allows validation of the concepts by comparison with experimental measurements. Thus, for binary flow, the integrated form of Eq. (37) can be written

$$\Delta p = \int_0^{\Delta X_1} \frac{F}{G}\,\mathrm{d}X_1 \tag{38a}$$

$$F = \frac{X_1}{(D_\mathrm{A})_{21}} - \frac{X_2}{(D_\mathrm{A})_{12}}\frac{\widetilde{J}_1}{\widetilde{J}_2} \quad G = -cA_\mathrm{A}\left[\frac{\widetilde{J}_1}{\widetilde{J}_2}\sqrt{M_1} + \sqrt{M_2}\right] \tag{38b}$$

For a known ΔX_1 and an assumed value of mean pore radius R, Eq. (38a) can be integrated numerically. If a starter value of $\widetilde{J}_1/\widetilde{J}_2$ is specified, a procedure can easily be devised whereby the flux ratio is adjusted until the correct value of Δp is obtained. By comparing theoretical and experimental values of flux ratio as described below, the mean pore radius R can be deduced. Knowing R, Eq. (34b) for a binary mixture can be integrated across the sample to give

$$\widetilde{J}_2 = -\frac{\varepsilon}{\tau^2 L}\int_{p(0)}^{p(L)} \left[A_\mathrm{A}\left(\frac{\widetilde{J}_1}{\widetilde{J}_2}\sqrt{M_1} + \sqrt{M_2}\right)\right]^{-1} \mathrm{d}p \tag{39}$$

and ε/τ^2 can be determined by comparison with absolute flux measurements. Alternatively, permeability measurements can be used for the same purpose. It is interesting to note that, for given R, Δp and ΔX_1, Eq. (39) predicts that the absolute fluxes are proportional to $\varepsilon/\tau^2 L$.

This procedure can be illustrated by reference to the experimental measurements of helium–argon counter-diffusion performed by Evans et al. [29–31]. The first paper describes flow measurements in 'specimen B' which was a porous graphite material with high permeability and large pore size, while the second and third papers describe experiments in 'specimen A' which was also graphite but had a much lower permeability and smaller pore size. Careful study of the published data shows that the measurements were extremely consistent and confirms the high reputation of the work. A full description of the experiments and tabulations of the data can be found in the papers.

Of particular interest are the experiments performed on specimen A at various mean pressures. Table IV of [30] lists 9 tests conducted with zero pressure difference across the sample ($\Delta p = 0$). However, as mentioned earlier, constant pressure tests cannot be used to deduce the mean pore radius because the square-root relation applies at both continuum and free-molecule limits and, according to the adopted interpolation procedure, at intermediate conditions also. Of more interest, therefore, are the measurements listed in Table I of [31] which refer to tests with both positive and negative pressure differences, performed at mean pressures of 1.49, 1.96, 2.97, 3.98 and 4.93 atm. CPIM calculations were performed for all the tests but only the results relating to the 1.49 and 4.93 atm experiments are presented here. Table I of [31] lists values of pressure difference Δp and it is stated in the text that the argon mole fraction difference was $\Delta X_\mathrm{Ar} = 0.963$. Apart from standard data required to calculate the viscosity and binary diffusion coefficients of helium–argon mixtures using the methods of Wilke and Fuller as described by Poling et al. [17], this is all the information required for the application of Eq. (38).

The results of the calculations are shown in Fig. 3 together with the experimental measurements of the molar

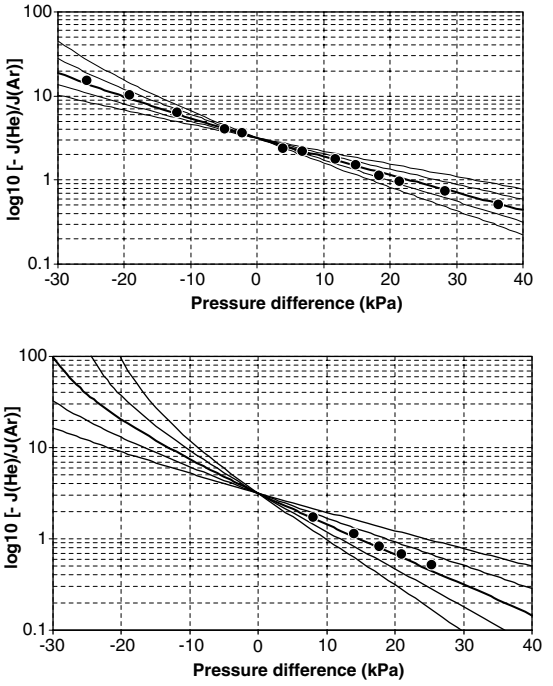

Fig. 3. Helium–argon counter-diffusion through graphite: Specimen A of Evans et al. [31]. Molar flux ratio versus pressure difference. Experimental data: solid circles. CPIM calculations for $R = 0.25$, 0.30, 0.35, 0.40, 0.45 μm. Mean pressure = 1.49 atm (top), 4.93 atm (bottom).

flux ratio $\widetilde{J}_{Ar}/\widetilde{J}_{He}$ obtained from the data of Table 1 in [31]. Fig. 3 shows tests at mean pressures of 1.49 atm and 4.93 atm. It can be seen that, contrary to common belief, it is perfectly possible to deduce a value of the mean pore radius from experimental determinations of the flux ratio so long as measurements with non-zero pressure gradient are available. Indeed, the various theoretical curves plotted show that R can be deduced with considerable accuracy. An interesting feature of this method of presentation is the crossing of the curves at $\Delta p = 0$ providing a graphic illustration of the indeterminacy of R at this condition. Good agreement was also obtained for the other tests not shown here and an overall assessment provided an estimate of $R = 0.35 \pm 0.02$ μm which is consistent with the description of specimen A given by Evans et al. [30].

Calculations of the absolute molar fluxes from Eq. (39) were then used to deduce the magnitude of the tortuosity using $R = 0.35$ μm and the values of $\varepsilon = 0.11$ and $L = 4.47$ mm given in [30]. The results, also for mean pressures of 1.49 and 4.93 atm, are shown in Fig. 4. As before, the consistency of the data is very good and an overall assessment at all pressures gives an estimate of $\tau = 28.5 \pm 1.0$. Although this seems very high for a tortuosity, the corresponding value of $\varepsilon/\tau^2 = 1.35 \times 10^{-4}$ is entirely consistent with the value of 1.42×10^{-4} quoted in Table III of [30].

As noted above, once the mean pore radius has been found, individual gas permeability measurements can also be used to deduce the value of ε/τ^2. Table II in [30] lists permeability data for helium at various pressures and these are plotted, together with data for argon, in Fig. 1 of Evans et al. [31]. CPIM calculations using Eq. (36) with $R = 0.35$ μm, $\varepsilon = 0.11$ and $\tau = 28.5$ were carried out and Fig. 5 shows a comparison of the results with the experimental data. Excellent agreement is displayed except for helium at very low pressures. As shown, these data points correspond to very high values of the *pressure* Knudsen number ($Kn_P = A_C/A_K$). This suggests that the free-molecule theory might need attention, although it should be noted that the argon data at similarly low pressures (but not quite so high Knudsen numbers) agree well with the theory.

The experimental results for specimen B are presented in Evans et al. [29] but the data are much less

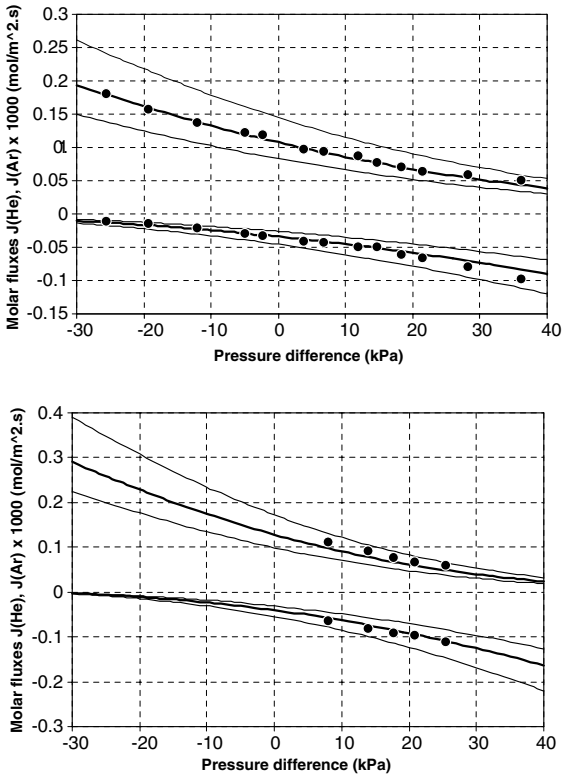

Fig. 4. Helium–argon counter-diffusion through graphite: Specimen A of Evans et al. [31]. Total molar fluxes versus pressure difference. Experimental data: solid circles. CPIM calculations for $R = 0.35$ μm and tortuosity = 25.0, 29.0, 33.0. Mean pressure = 1.49 atm (top), 4.93 atm (bottom).

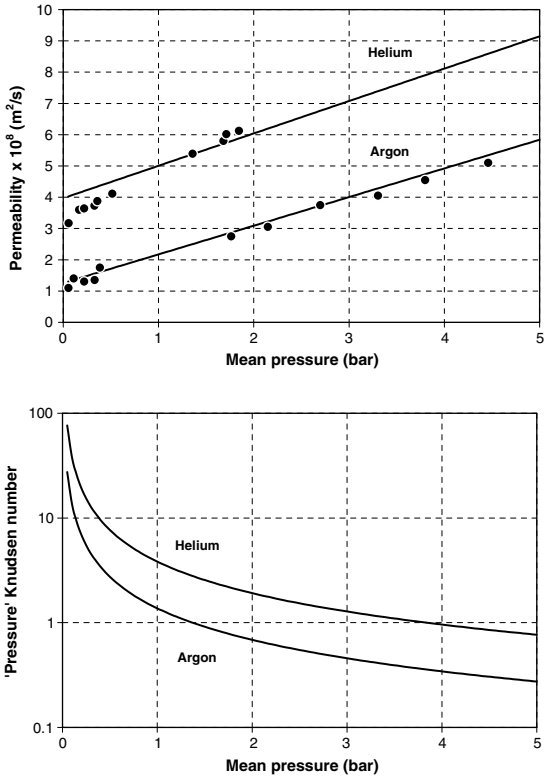

Fig. 5. Permeability of helium and argon in specimen A of Evans et al. [30,31]. CPIM calculations for $R = 0.35$ μm, $\varepsilon = 0.11$, $\tau = 28.5$. Experimental data: solid circles. 'Pressure' Knudsen number defined by $Kn_P = A_C/A_K$.

extensive than for specimen A. The porosity was measured as $\varepsilon = 0.22$ and the specimen thickness was $L = 3.80$ mm. 18 constant pressure tests are listed in Tables I and II of the paper but there are only 4 tests with non-zero Δp. CPIM calculations for these tests using Eqs. (38) and (39) gave $R = 3.74$, 3.82, 3.92 and 4.02 μm, and $\tau = 4.95$, 4.99, 5.04 and 4.88. Despite the minimal data, these values are very consistent and the tortuosity agrees closely with the value 5.08 quoted in the paper.

8. Summary and conclusions

In developing the CPIM, the original intention was to clarify the theory of multi-component diffusive flow in porous materials. What has emerged, however, is a unified treatment which provides a more satisfactory way of interpreting the empirical parameters and equations characterising flow in such a medium.

Continuum diffusion in capillaries has been dealt with in some detail. A most important aspect is the wall boundary condition as this is the source of Graham's square-root law of diffusion. A re-examination based on Sutherland's theory of momentum transport in gas mixtures (Appendix 1) gives the same continuum solution as the original theory (Eq. (5)). Further progress will require more elaborate approaches based on the Boltzmann equation.

The Stefan–Maxwell species-momentum equations have also been re-examined and recast in a form highlighting the approximations involved in their derivation (Appendix 2). It is concluded that modelling the neglected shear stress terms simply complicates the analysis without providing any proven advantage. Integration of the Stefan–Maxwell equations over the pore cross-section shows that the local and pore-averaged forms are identical (Eq. (9)), an extremely useful result which would be lost if extra terms are included. The analysis is completed by application of the force–momentum principle giving the pressure gradient in terms of the component fluxes (Eq. (13)). The special case of binary flow has been discussed and examples of flux profiles with diffusion slip are given in Fig. 2.

The treatment of free-molecule flow is standard, but the algebraic re-arrangement to give Eqs. (20) and (22) is not. These equations are identical in form to Eqs. (13) and (9) for continuum flow and it is this correspondence which underpins the interpolation procedure to arrive at Eqs. (27) and (31) for flow at arbitrary Knudsen numbers. The method of derivation is unambiguous and there is no question of introducing further *viscous* or *bulk flow* terms as is seen so often in the literature.

The extension to flow in porous solids is achieved in the usual way by introducing the porosity and tortuosity which combine into a single factor ε/τ^2. Unlike other treatments, however, this factor is not absorbed into the gas diffusivities and flow permeability. Instead, it is shown that ε/τ^2 can be eliminated between the Stefan–Maxwell and pressure gradient equations to give the fascinating prediction that the flux *ratios* are defined completely by the mean pore radius and inlet/outlet boundary conditions, and are independent of ε and τ. It is only the absolute flux magnitudes which depend on ε/τ^2 and this parameter acquires a much clearer physical significance when it is viewed as a scaling factor for the length co-ordinate rather than a modifier of the gas diffusivities. In the CPIM theory, the latter depend only on the mean pore radius R.

For clarification and validation purposes, CPIM calculations have been compared with the extensive experimental data of helium–argon counter-diffusion obtained by Evans et al. [29–31]. As shown in Figs. 3–5, the agreement between theory and measurement is extremely good. In particular, it has been shown that, contrary to common belief, very consistent estimates of the mean pore radius can be obtained by measuring flux ratios at non-zero pressure differences. It is only for the special case of constant pressure counter-diffusion that the evaluation of the mean pore radius is indeterminate.

It is hoped that the work described in this paper not only clarifies the theory of diffusion in capillaries and porous solids but also indicates a more effective way of approaching experimental data analysis and the interpretation of the empirical parameters used to describe flows in porous solids. There are clearly many interesting avenues to explore using this type of approach in investigating the behaviour of more complex multi-component mixtures both with and without chemical reaction.

Appendix 1. Sutherland's viscosity theory and the wall boundary condition

The mean free path of an s-molecule is given by

$$\lambda_s = \bar{w}_s \left[\sum_r \nu_{sr} \right]^{-1} \tag{A1.1}$$

where $\bar{w}_s$ is the mean speed of an s-molecule and ν_{sr} is the collision frequency between the r-molecules and a given s-molecule. From equilibrium kinetic theory,

$$\bar{w}_s = \left(\frac{8 R_g T}{\pi M_s} \right)^{1/2} \tag{A1.2}$$

and, for hard sphere molecules,

$$\nu_{sr} = n_r \sigma_{sr}^2 \left[8\pi R_g T \left(\frac{1}{M_s} + \frac{1}{M_r} \right) \right]^{1/2} \tag{A1.3}$$

where n_r is the r-molecule number density and σ_{sr} is the mean diameter of s- and r-molecules. It should be noted

that Eq. (A1.3) holds also for $r \equiv s$, see Chapman and Cowling [32].

Sutherland considered the viscosity of a non-diffusing gas mixture. With reference to Fig. A1.1, his approach is equivalent to the assumption that, before crossing the plane $y = 0$, each s-molecule makes its last collision at a distance $l_s = C\lambda_s$ above or below the plane. It is also assumed (the weakest part of the theory) that each molecule acquires there, on average, the local value of the species velocity. Performing the analysis just as for a single-component gas, see Chapman and Cowling [32], the dynamic viscosity of a gas mixture μ follows as

$$\mu = \sum_s \left(\frac{\rho_s \bar{w}_s \lambda_s}{2} \right) \tag{A1.4}$$

where C is assumed to be unity to conform with the Chapman–Enskog hard sphere result for a single-component gas. Eq. (A1.4) is a generalised version of Eq. (8) of Sutherland [15]. Using Eqs. (A1.1)–(A1.3), it can be manipulated into the form

$$\mu = \sum_s \left[X_s \mu_s / \sum_r X_r \alpha_{sr} \right] \tag{A1.5}$$

where μ_s is the viscosity of pure species-s at the same temperature and the α_{sr} are given by

$$\alpha_{sr} = \left(\frac{\sigma_{sr}}{\sigma_{ss}} \right)^2 \left(\frac{M_s + M_r}{2M_r} \right)^{1/2} \tag{A1.6}$$

In practice, Sutherland found that Eq. (A1.5) needed empirical adjustment to give agreement with experimental data. He therefore replaced the α_{sr} by $\phi_{sr}\alpha_{sr}$ where $\phi_{sr} = [2M_r/(M_s + M_r)]^m$ with $m = 0.75$. Later work by Wilke [16] suggested that $m = 1$ gave better accuracy. With this modification, the viscosity is still given by Eq. (A1.4) if λ_s is taken as

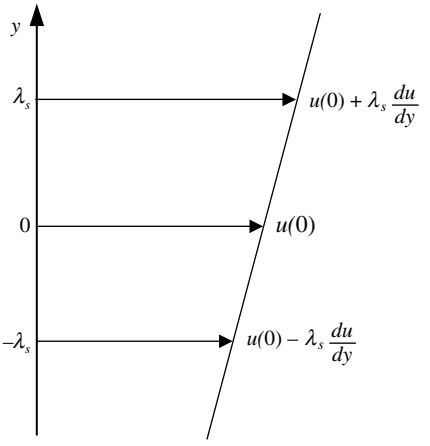

Fig. A1.1. Illustrating viscosity analysis in the bulk: s-molecules make their last collision around $y = \pm\lambda_s$ before crossing the plane $y = 0$.

$$\lambda_s = \bar{w}_s \left[\sum_r \phi_{sr} v_{sr} \right]^{-1} \tag{A1.7}$$

Consider now the flow of a gas mixture over a solid wall with velocity gradients normal to, and concentration gradients parallel to, the wall (Fig. A1.2). The assumption is made that s-molecules make their last collision before impacting the wall at $y = C\lambda_s$ with λ_s given by Eq. (A1.7) and $C = 1$ (for consistency with the above theory). It is also assumed that each s-molecule acquires the average species velocity at this location. This velocity is given by $[u_{s,w} + \lambda_s(\partial u_s/\partial y)_w]$ where $u_{s,w}$ is the *effective* wall slip velocity of component s and $(\partial u_s/\partial y)_w$ is the *effective* gradient of u_s at the wall. Noting that the molecular mass flux to a surface is $\rho_s \bar{w}_s/4$, the streamwise momentum flux lost to the wall by impacting s-molecules is

$$f_s \frac{\rho_s \bar{w}_s}{4} \left[u_{s,w} + \lambda_s \left(\frac{\partial u_s}{\partial y} \right)_w \right] \tag{A1.8}$$

where f_s is the *diffuse reflection coefficient*. Summing over all components gives the total momentum flux lost to the wall which, in macroscopic terms, is the wall shear stress τ_w. Then, assuming that the shear stress remains constant out into the continuum region, it follows that

$$\tau_w = \sum_s f_s \frac{\rho_s \bar{w}_s}{4} \left[u_{s,w} + \lambda_s \left(\frac{\partial u_s}{\partial y} \right)_w \right] = \mu \left(\frac{\partial u_m}{\partial y} \right)_w \tag{A1.9}$$

where u_m is the mass-mean velocity and μ is the dynamic viscosity of the gas mixture.

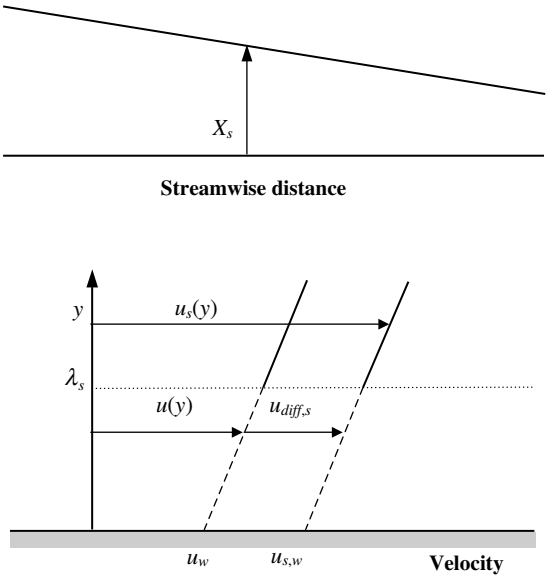

Fig. A1.2. Illustrating the wall boundary analysis: s-molecules make their last collision around $y = \lambda_s$ before impacting the wall at $y = 0$. Dotted lines represent extrapolations to the wall.

For Poiseuille flow, the $u_{\mathrm{diff},s}$ are constant across the tube. Hence $\partial u_{\mathrm{diff},s}/\partial y = 0$ and $\partial u_s/\partial y = \partial u_m/\partial y$. Using this relationship and Eq. (A1.4) for μ (i.e., assuming the viscosity is unchanged by simultaneous diffusion):

$$\sum_s f_s \rho_s \bar{w}_s u_{s,\mathrm{w}} = \sum_s (2 - f_s)\rho_s \bar{w}_s \lambda_s \left(\frac{\partial u_m}{\partial y}\right)_{\mathrm{w}} \tag{A1.10}$$

It should be noted that the Sutherland model only enters via Eq. (A1.7) for λ_s. Eq. (A1.10) is valid for slip flow but here the interest is in the continuum limit where it becomes

$$\sum_s f_s \rho_s \bar{w}_s u_{s,\mathrm{w}} = \sum_s f_s M_s c_s \bar{w}_s v_{s,\mathrm{w}} = 0 \tag{A1.11}$$

Introducing G_s and J_s from Eq. (4), noting that $G_{s,\mathrm{w}} = G_{\mathrm{w}} + G_{\mathrm{diff},s}$ and $J_{s,\mathrm{w}} = J_{\mathrm{w}} + J_{\mathrm{diff},s}$ and substituting Eq. (A1.2) leads to Eq. (5) in the main text if it is assumed that the f_s are all the same.

Appendix 2. The species momentum equation

The momentum equation for gas species-s is best obtained directly from kinetic theory as this emphasises the approximations involved. Working in three space dimensions, the i-component of velocity of a molecule of species-s is denoted by $(c_s)_i$ and this is represented in the conventional way as the sum of the i-component mass-mean velocity $(u_m)_i$ and a random velocity $(C_s)_i$. Thus:

$$(c_s)_i = (u_m)_i + (C_s)_i \tag{A2.1}$$

and the mean values of $(c_s)_i$ and $(C_s)_i$ are $(u_s)_i$ and $(u_{\mathrm{diff},s})_i$, respectively (see after Eq. (4)).

A clear derivation from the Boltzmann equation of the species mass and momentum conservation equations is given by Vincenti and Kruger [33]. Using the present notation with the Einstein summation convention, the equations are (in the absence of body forces):

$$\frac{\partial \rho_s}{\partial t} + \frac{\partial}{\partial x_j}[\rho_s (u_s)_j] = 0 \tag{A2.2a}$$

$$\frac{\partial}{\partial t}[\rho_s (u_s)_i] + \frac{\partial}{\partial x_j}[\rho_s \overline{(c_s)_i (c_s)_j}] = \sum_r \Delta_{sr}[m_s c_i] \tag{A2.2b}$$

where the term on the right hand side of Eq. (A2.2b) represents the momentum transferred to the s-molecules by collisions with molecules of all other species.

Substituting Eqs. (A2.1) and (A2.2a) into (A2.2b) gives, after some manipulation,

$$\rho_s \frac{D(u_m)_i}{Dt} + \frac{D(G_{\mathrm{diff},s})_i}{Dt} + (G_{\mathrm{diff},s})_i \frac{\partial (u_m)_j}{\partial x_j} + (G_{\mathrm{diff},s})_j \frac{\partial (u_m)_i}{\partial x_j} = \frac{\partial (\tau_s)_{ij}}{\partial x_j} - \frac{\partial p_s}{\partial x_i} + \sum_r \Delta_{sr}[m_s c_i] \tag{A2.3}$$

where $D/Dt = \partial/\partial t + (u_m)_j \partial/\partial x_j$, $(G_{\mathrm{diff},s})_i = \rho_s (u_{\mathrm{diff},s})_i$ is the i-component of the diffusive mass flux, and $(\tau_s)_{ij}$ is the contribution to the viscous shear stress from the s-molecules formally given by

$$(\tau_s)_{ij} = -\rho_s \overline{(C_s)_i (C_s)_j} + p_s \delta_{ij} \tag{A2.4}$$

Summing over all components gives, as expected, the overall momentum equation:

$$\rho \frac{D(u_m)_i}{Dt} = \frac{\partial \tau_{ij}}{\partial x_j} - \frac{\partial p}{\partial x_i} \tag{A2.5}$$

where τ_{ij} is the summation over all species of the $(\tau_s)_{ij}$.

Multiplying Eq. (A2.5) by the mass fraction Y_s, subtracting from Eq. (A2.3) and using the identity $p_s = X_s p$ gives the required *exact* form of the species momentum equation:

$$\frac{D(G_{\mathrm{diff},s})_i}{Dt} + (G_{\mathrm{diff},s})_i \frac{\partial (u_m)_j}{\partial x_j} + (G_{\mathrm{diff},s})_j \frac{\partial (u_m)_i}{\partial x_j} + (X_s - Y_s)\frac{\partial p}{\partial x_i} + p\frac{\partial X_s}{\partial x_i} + \left[Y_s \frac{\partial \tau_{ij}}{\partial x_j} - \frac{\partial (\tau_s)_{ij}}{\partial x_j}\right] = \sum_r \Delta_{sr}[m_s c_i] \tag{A2.6}$$

Each term of Eq. (A2.6) sums over s independently to zero.

The simplest case is when all velocity gradients are zero. Chapman–Enskog theory then provides an expression for the term on the right hand side and Eq. (A2.6) takes the form

$$p\frac{\partial X_s}{\partial x_i} + (X_s - Y_s)\frac{\partial p}{\partial x_i} = R_{\mathrm{g}} T \sum_r \left[\frac{X_s J_r}{(D_{\mathrm{B}})_{rs}} - \frac{X_r J_s}{(D_{\mathrm{B}})_{sr}}\right] \tag{A2.7}$$

where in the first Chapman–Enskog approximation, $(D_{\mathrm{B}})_{rs} = (D_{\mathrm{B}})_{sr}$ is the binary diffusion coefficient of a s–r gas mixture. Neglecting *pressure diffusion* (the second term of Eq. (A2.7)) results in the basic form of the Stefan–Maxwell equations.

When the velocity gradients are non-zero the question arises as to whether or not Eq. (A2.7), with or without pressure diffusion, should be modified. In other words, does viscous momentum transfer have a significant effect on diffusive mass transfer? Plainly, there is *some* effect because of the extra terms which now appear in Eq. (A2.6) and because the collisional momentum transfer term also needs modification. Whether or not these effects are significant, however, is an altogether different matter.

Attempts have been made to include viscous momentum transfer in the species momentum equation, most notably by Kerkof [9] and Kerkof et al. [10]. However, because of the rather ad hoc derivations, it is difficult to assess the validity of the modelling in these papers. For example, in their VPM theory, Kerkhof et al. [10] start with Eq. (A2.3), ignoring all terms on the left hand side completely while introducing a model for $\partial(\tau_s)_{ij}/\partial x_j$ which really requires more justification than is supplied. Because of this term, the subsequent analysis becomes very complicated and the physics is obscured.

The present authors believe that if modifications are to be introduced they should be based on Eq. (A2.6). In these equations, the shear stress difference terms in square brackets are clearly non-zero. However, whether or not they have an appreciable overall effect will only be revealed by detailed physical modelling in combination with more accurate and extensive experimental measurements. Given our current capability for modelling flow in porous solids, it is felt that corrections to the basic form (without pressure diffusion) of Eq. (A2.7) cannot yet be justified. What is certainly true is that the additional complexity of the resulting analysis is highly undesirable.

References

[1] B.A. Haberman, J.B. Young, Three-dimensional simulation of chemically reacting gas flows in the porous support structure of an integrated-planar solid oxide fuel cell, Int. J. Heat Mass Transfer 47 (2004) 3617–3629.

[2] R.B. Evans, G.M. Watson, E.A. Mason, Gaseous diffusion in porous media at uniform pressure, J. Chem. Phys. 35 (1961) 2076–2083.

[3] R.B. Evans, G.M. Watson, E.A. Mason, Gaseous diffusion in porous media. II—effect of pressure gradients, J. Chem. Phys. 36 (1962) 1894–1902.

[4] E.A. Mason, A.P. MalinauskasGas Transport in Porous Media, Chemical Engineering Monographs, vol. 17, Elsevier, Amsterdam, 1983.

[5] L.B. Rothwell, Gaseous counterdiffusion in catalyst pellets, Am. Inst. Chem. Eng. J. 9 (1963) 19–24.

[6] P. Schneider, Multicomponent isothermal diffusion and forced flow of gases in capillaries, Chem. Eng. Sci. 33 (1978) 1311–1319.

[7] D. Arnost, P. Schneider, Dynamic transport of multicomponent mixtures of gases in porous solids, Chem. Eng. J. 57 (1995) 91–99.

[8] R. JacksonTransport in Porous Catalysts, Chemical Engineering Monographs, vol. 4, Elsevier, Amsterdam, 1977.

[9] P.J.A.M. Kerkhof, A modified Maxwell–Stefan model for transport through inert membranes: the binary friction model, Chem. Eng. J. 64 (1996) 319–343.

[10] P.J.A.M. Kerkhof, M.A.M. Geboers, K.J. Ptasinski, On the isothermal binary mass transport in a single pore, Chem. Eng. J. 83 (2001) 107–121.

[11] D.B. Spalding, Combustion and Mass Transfer, Pergamon, 1979.

[12] H.A. Kramers, J. Kistemaker, On the slip of a diffusing gas mixture along a wall, Physica 10 (1943) 699–713.

[13] A.F. Mills, On steady one-dimensional diffusion in binary ideal gas mixtures, Int. J. Heat Mass Transfer 46 (2003) 2495–2497.

[14] E.H. Kennard, Kinetic Theory of Gases, McGraw-Hill, 1938, pp. 295–298 and 302–306.

[15] W. Sutherland, The viscosity of mixed gases, Philos. Mag. 40 (1895) 421–431.

[16] C.R. Wilke, A viscosity equation for gas mixtures, J. Chem. Phys. 18 (1950) 517–519.

[17] B.E. Poling, J.M. Pausnitz, J.P. O'Connell, The Properties of Gases and Liquids, fifth ed., McGraw-Hill, 2001, Sections 9.5 and 11.4.

[18] G. Mo, F. Rosenberger, Molecular-dynamics simulations of flow with binary diffusion in a two-dimensional channel with atomically rough walls, Phys. Rev. A 44 (1991) 4978–4985.

[19] T. Kanki, S. Iuchi, Y. Yamamoto, Diffusion of rarefied gas mixtures in a circular tube under the existence of pressure gradients, Phys. Fluids 23 (1980) 1501–1509.

[20] S. Takata, S. Yasuda, S. Kosuge, K. Aoki, Numerical analysis of thermal-slip and diffusion-slip flows of a binary mixture of hard-sphere molecular gases, Phys. Fluids 15 (2003) 3745–3766.

[21] F. Sharipov, D. Kalempa, Velocity slip and temperature jump coefficients for gaseous mixtures. III. Diffusion slip coefficient, Phys. Fluids 16 (2004) 3779–3785.

[22] H. Lang, S.K. Loyalka, An exact expression for the diffusion slip velocity in a binary gas mixture, Phys. Fluids 13 (1970) 1871–1873.

[23] J.O. Hirshfelder, C.F. Curtis, R.B. Bird, Molecular Theory of Gases and Liquids, Wiley, 1954, pp. 514–520.

[24] F.A.L. Dullien, D.S. Scott, The flux-ratio for binary counterdiffusion of ideal gases, Chem. Eng. Sci. 17 (1962) 771–775.

[25] J. Hoogschagen, Diffusion in porous catalysts and adsorbents, Ind. Eng. Chem. 47 (1955) 906–913.

[26] D.S. Scott, K.E. Cox, Temperature dependence of the binary diffusion coefficient of gases, Can. J. Chem. Eng. 38 (1960) 201–205.

[27] W.G. Pollard, R.D. Present, On gaseous self-diffusion in long capillary tubes, Phys. Rev. 73 (1948) 762–774.

[28] N. Epstein, On tortuosity and the tortuosity factor in flow and diffusion through porous media, Chem. Eng. Sci. 44 (1989) 777–779.

[29] R.B. Evans, J. Truitt, G.M. Watson, Interdiffusion of helium and argon in a large-pore graphite, J. Chem. Eng. Data 6 (1961) 522–525.

[30] R.B. Evans, G.M. Watson, J. Truitt, Interdiffusion of gases in a low permeability graphite at uniform pressure, J. Appl. Phys. 33 (1962) 2682–2688.

[31] R.B. Evans, G.M. Watson, J. Truitt, Interdiffusion of gases in a low permeability graphite. II—influence of pressure gradients, J. Appl. Phys. 34 (1963) 2020–2026.

[32] S. Chapman, T.G. Cowling, The Mathematical Theory of Non-uniform Gases, third ed., Cambridge University Press, 1970, pp. 70 and 97.

[33] W.G. Vincenti, C.H. Kruger Jr., Introduction to Physical Gas Dynamics, Krieger, 1967, pp. 368–373.